

**Joel Guidez<sup>1</sup>**

CEA,  
CEN Saclay,  
GIF/Yvette 91190, France  
e-mail: joel.guidez@cea.fr

**Janos Bodi**

Paul Scherrer Institut,  
Villigen PSI 5232, Switzerland  
e-mail: janos.bodi@psi.ch

**Konstantin Mikityuk**

Mem. ASME  
Paul Scherrer Institut,  
Villigen PSI 5232, Switzerland  
e-mail: konstantin.mikityuk@psi.ch

**Enrico Girardi**

EDF Lab Paris-Saclay,  
7, Boulevard Gaspard Monge,  
Palaiseau 91120, France  
e-mail: enrico.girardi@edf.fr

**Jeremy Bittan**

EDF Lab Paris-Saclay,  
7, Boulevard Gaspard Monge,  
Palaiseau 91120, France  
e-mail: jeremy.bittan@edf.fr

**Aleksander Grah**

Joint Research Center—Petten,  
P.O. Box 2,  
Petten NL-1755 ZG, The Netherlands  
e-mail: Aleksander.GRAH@ec.europa.eu

**Haileyesus Tsige-Tamirat**

Joint Research Center—Petten,  
P.O. Box 2,  
Petten NL-1755 ZG, The Netherlands  
e-mail: Haileyesus.TSIGE-  
TAMIRAT@ec.europa.eu

**Pablo Romojaro<sup>2</sup>**

CIEMAT,  
Avda. Complutense, 40. Ed. 17,  
Madrid 28040, Spain  
e-mails: pablo.romojaro@ciemat.es;  
pablo.romojaro@sckcen.be

**Francisco Álvarez-Velarde**

CIEMAT,  
Avda. Complutense, 40. Ed. 17,  
Madrid 28040, Spain  
e-mail: francisco.alvarez@ciemat.es

**Bernard Carlucci**

FRAMATOME,  
10 rue Juliette Récamier,  
Lyon Cedex 06 69456, France  
e-mail: bernard.carlucci@framatome.com

# New Reactor Safety Measures for the European Sodium Fast Reactor—Part II: Preliminary Assessment

*The European Sodium Fast Reactor Safety Measures Assessment and Research Tools (ESFR-SMART) project offers innovative options for a sodium fast reactor (SFR) to improve its safety. This paper explains the preliminary calculations made on the main options to roughly verify their feasibility. Design propositions and calculations are here provided of the following innovative options: elimination of the safety vessel, innovative decay heat removal systems (DHRS), core catcher, thermal pumps, and secondary loops. In conclusion, all these options seem able to fulfill the key points of new safety rules for Generation-IV reactors. A status of the research and development (R&D) effort necessary to validate these new options is also proposed. [DOI: 10.1115/1.4051723]*

<sup>1</sup>Corresponding author.

<sup>2</sup>Present address: SCK-CEN, Boeretang 200, Mol 2400, Belgium.

Manuscript received July 7, 2020; final manuscript received June 30, 2021; published online August 12, 2021. Assoc. Editor: Joerg Starflinger.

## 1 Introduction

European Sodium Fast Reactor Safety Measures Assessment and Research Tools (ESFR-SMART) project [1] is a “working horse” which offers options on the design of a fast sodium reactor to improve its safety. These options are not validated, as in an industrial project, by design and manufacturing studies by the manufacturer in charge. Similarly, these proposals are not validated by an analysis of the safety authorities. However, it appeared necessary to verify them by appropriate precalculations to demonstrate that the order of magnitude of the parameters was correct, and that the key points of the feasibility were assured.

The paper consists of two parts. Part I presents the main options of the 1500 MW<sub>el</sub> pool ESFR concept [2] as proposed by the ESFR-SMART project [1], while the current Part II presents preliminary assessment of the newly proposed safety measures.

The paper is structured according to the five main innovative options introduced in the design with respect to the previous ESFR [3], aimed at introducing more safety, simplification (simplicity and safety of plant operation, economy), and passivity (more robust safety demonstration) in the reactor architecture, and for which a preliminary assessment was provided:

- elimination of the safety vessel
- new decay heat removal systems (DHRS)
- core catcher system
- thermal pumps
- optimization of secondary loops

The remaining uncertainties are mentioned and, finally, a summary of the points requiring additional research and development (R&D) is proposed in conclusion.

## 2 Elimination of the Safety Vessel

All existing sodium fast reactors (SFRs) operated in the world featured a safety vessel (see as an example, Fig. 1, the Superphénix safety vessel [4]) around the main vessel. The function of this safety vessel is to contain the primary sodium in case of the main vessel leakage. For ESFR-SMART, the goal is to avoid lowering of the primary sodium free level below the inlet windows of the intermediate heat exchangers (IHXs) and thus providing an efficient sodium circulation through the core. In case of the main vessel leakage, the reactor is not recoverable, and the core must be unloaded. Due to the need to wait for reduction of the decay core heat, this handling takes at least one year. The safety vessel must therefore remain filled with sodium for a long time. The potential danger in these conditions is that the reactor pit is not designed to withstand a sodium leak from the safety vessel. Moreover, a sodium leak from the safety vessel would also lead to interruption of the sodium circulation through the IHXs, leading to a more difficult overall situation. The scenarios of vessel leakage are diverse, from corrosion leakage (as for the main vessel of the Superphénix storage drum [4]) to leakage on a severe accident with mechanical energy release. This leads to high uncertainties in the temperatures and leakage rates, which make it difficult to assess the safety vessel mechanical strength against the corresponding thermal shocks.

So, the safety vessel is a proven option, especially demonstrated during the incident at the Superphénix storage drum, and is adopted in all existing reactors. However, the evolution of safety standards leads us to look at other options where its functions could be directly taken over by a reactor pit capable of withstanding a sodium leak, and thus a long-term mitigation situation. It was an option that had already been looked at in the European Fast Reactor project with a vessel anchored in the pit, which option was later abandoned for reasons of feasibility and design difficulties.

**2.1 General Description of the Reactor Pit Design Proposed in the European Sodium Fast Reactor Safety Measures Assessment and Research Tools Project.** For ESFR-SMART, the goal is to practically eliminate the large primary sodium leak



**Fig. 1 Arrival of the safety vessel inside the reactor pit of Superphénix**

which could lead to core uncoolability. This is done by the implementation of both a steel liner on the reactor pit concrete and concrete inert to sodium. According to these design choices, the implementation of a safety vessel is no more needed. This innovative design must maintain the capability to inspect the reactor vessel welds.

The proposed design of the reactor pit is composed of the following domains (see Figs. 2 and 3):

- A mixed concrete/metal structure with a water cooling system inside the concrete supports the thick metal slab to which the reactor vessel is attached. Together with the reactor roof, it provides a sealed containment, which must keep its integrity in all the cases of normal or accidental operations.
- Inside the concrete/metal structure, blocks of insulating materials (nonreactive with sodium) are installed. Alumina is selected as reference material for the insulation blocks. A conventional insulation layer could be considered in future to increase insulation effects (outside the scope of the paper).
- A metallic liner is placed on the surface of the insulation blocks. The gap between the reactor vessel and the liner must be small enough (0.5 m was chosen) to avoid decrease of the primary sodium free level below the IHX windows in case of sodium leakage from the reactor vessel. During normal operation, the primary sodium free level is 1.35 m below the roof. In case of primary sodium leak, about 440 m<sup>3</sup> of sodium will leave the reactor vessel to fill the gap, and the new equilibrium free level of the primary sodium will be about 3.81 m below the reactor roof. With this level of sodium inside the primary circuit, there is still a 0.35 m sodium level above the upper IHX openings, which allows a sodium inflow into the IHX and a good natural convection and core cooling.
- The oil cooling system is installed next to or even inside the liner (Fig. 2).
- Finally, a special concrete with alumina (aluminous concrete) which could withstand, without significant chemical reaction with sodium, a leakage of the liner could be used between the liner and the insulation (blocks of alumina). This option however is out of scope of the current study.

Two independent active cooling systems are proposed in the reactor pit (we use the acronyms DHRS-3 for the combination of these two systems):

- The oil cooling system (DHRS-3.1) close to the liner (Fig. 4(a)). The oil under forced convection can remove the heat transferred by radiation from the reactor vessel at high temperature. Conversely to water, the adopted synthetic oil is resistant to high temperatures above 300 °C and reacts with

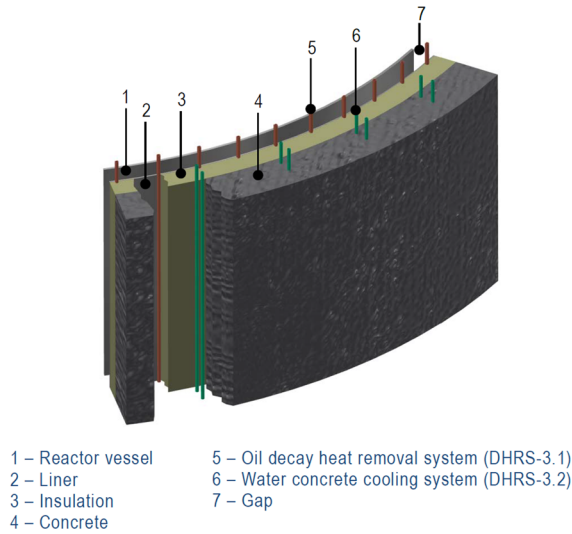


Fig. 2 Detail of the reactor pit design

sodium without hydrogen production. As an example, the “Therminol” commercial oil (“Therminol SP” [5] or “Therminol 59–62” [6]) can be used in normal operation at temperatures up to 315–325 °C.

- The water cooling system (DHRS-3.2) for the concrete cooling is installed in the concrete (Fig. 4(b)). It is not necessary for normal operating situation. Its aim is to maintain the concrete temperature under 70 °C in all accidental situations. For example, in case of severe accident and if we suppose that the DHRS-3.1 is lost.

Both oil and water circuits work during normal operation and have to maintain the concrete temperature below 70 °C. This margin is intended to ensure the concrete integrity and to protect it from thermal degradation. During the reactor shutdown, the oil system alone has to be able after few days to remove all the decay heat (DH) generated by the fuel. In case of the reactor vessel leak and loss of the oil system, the water system should be able to remove the DH generated by the core and to maintain the concrete below 70 °C.

**2.2 Main Design-Basis Scenarios.** The reactor pit must be designed for the following three main scenarios:

- **Scenario 1: Normal operation:** The main vessel is at about 400 °C. The operation of the oil cooling system should be sufficient to maintain the correct thermal conditions in the pit (i.e., less than 70 °C for the concrete of the mixed structures).
- **Scenario 2: Operation in exceptional DH removal regime:** The safety studies should also take into account accidental situations of successive losses of DHRS. In such exceptional situations, the reactor vessel is allowed to reach temperature of 650 °C. The two cooling systems (oil and water) must keep the concrete temperature below 70 °C, while playing an important role in the DH removal.
- **Scenario 3: Operation in accident situation of sodium leakage:** In this situation, strong sodium cooling is possible with the redundant and available DHRS, to bring the sodium to a temperature corresponding to the handling temperature (180 °C). Therefore, the maximum temperature of the sodium in the gap should not exceed 200 °C. The demonstration of the oil cooling system availability in case of reactor vessel leakage is difficult, and we assume as hypothesis that the oil cooling system is no longer available. The operation of the water cooling system alone must be sufficient to maintain the concrete temperature below 70 °C.

**2.3 Numerical Heat Transfer Model.** The objective is the development of a simple computational fluid dynamics (CFD) model to compute the steady-state heat transfer from the reactor vessel through the reactor pit. The CFD computations were performed with the ANSYS CFX code [7], which is a parallelized high-performance CFD software tool. It is based on finite volume technique applied to solve the Navier–Stokes equations. To achieve results with low computation time, the reactor pit is divided into 12 symmetrical sections (5 cm height), and the CFD analysis is performed for the resulting 30 deg section. The drawing of the geometry for one section, the “elementary cell” of the reactor pit structure, is shown on Fig. 5. For the calculation example, the oil cooling system is installed inside the liner of the special wavy shape (see Fig. 6).

The following simplifications and assumptions are applied at this stage of computations:

- The gap between the reactor vessel and the liner is considered as vacuum for first CFD computations to minimize the computational time.
- The material of the insulation layer is assumed to be glass wool for the current study.

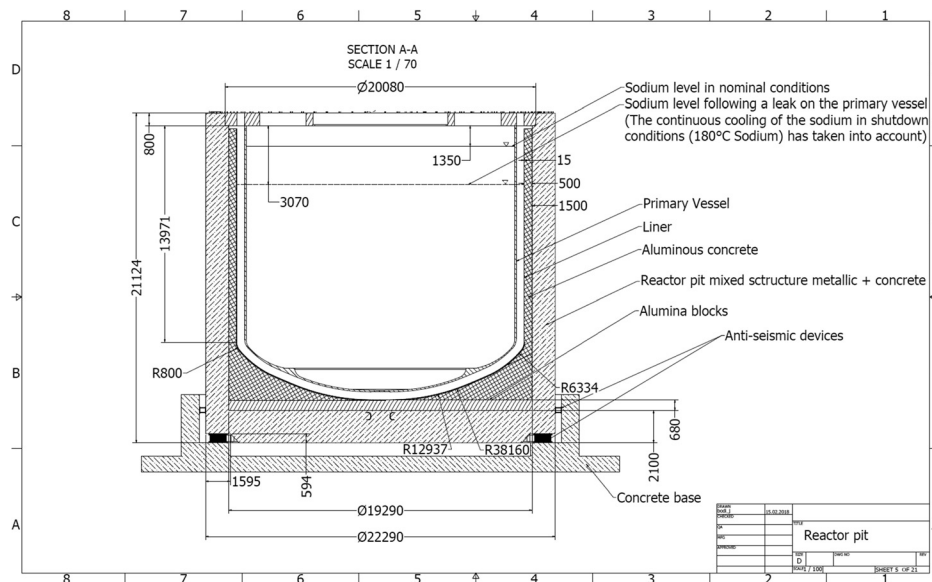
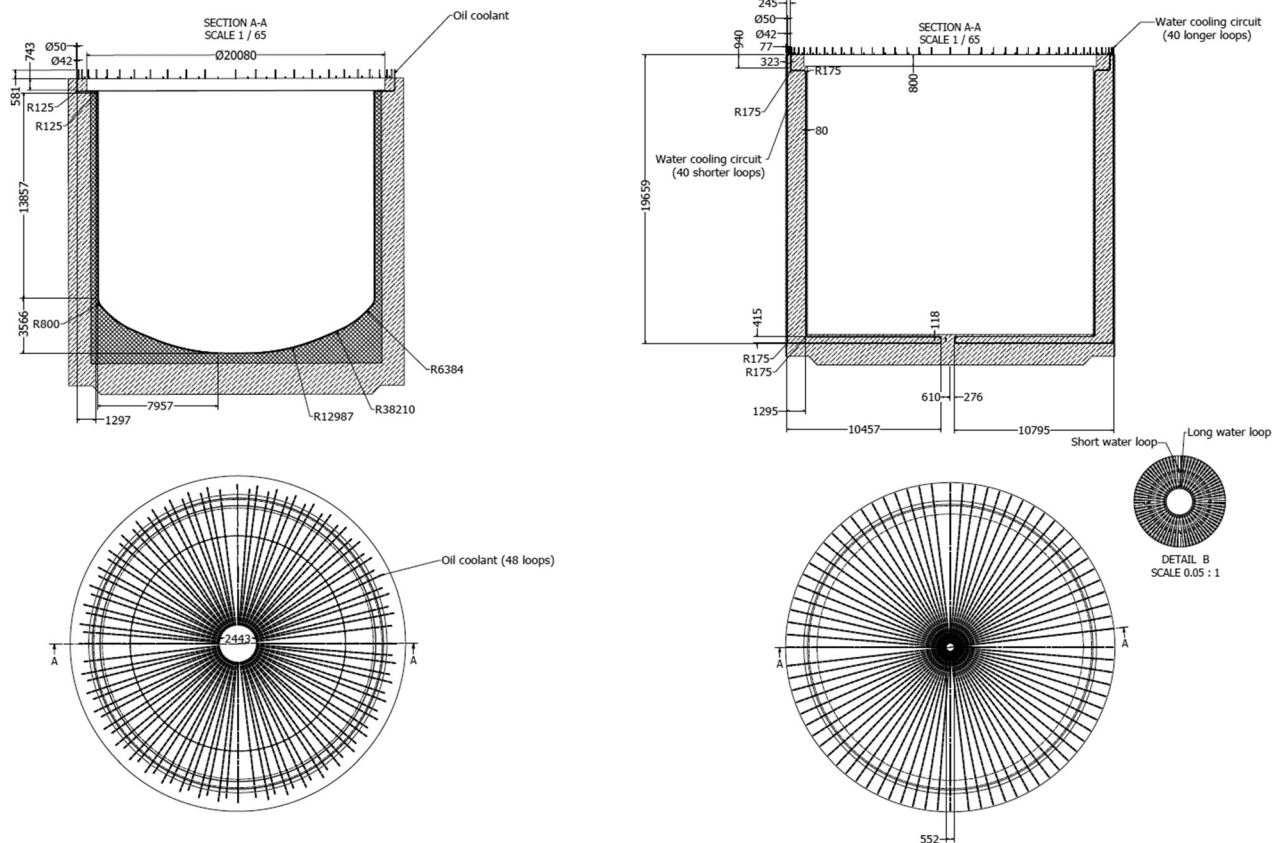


Fig. 3 Drawing of the reactor pit design





**Fig. 4 Drawings of the reactor pit cooling systems: DHRS-3.1 (left) and DHRS-3.1 (right)**

- Only steady-state computations are performed.

Fast solution is important (computation time below a minute) to be able to perform the large amounts of parametric studies. The resulting CFD model geometry is shown in Fig. 6. The domains for the CFD model in Fig. 6 are as follows ( $\lambda$  is the thermal conductivity) from left-hand to right-hand

- The outer surface of the reactor vessel wall is shown on the left-hand side.
- The gas gap;  $\lambda = 0.026$  W/m K. For the steady-state computations, the heat transport parameters (density and specific heat) are set to very low values, and the solution of the flow is switched off.
- The stainless steel liner of the wavy shape is proposed (blue);  $\lambda = 60.5$  W/m K with the pipes of the oil cooling system inside.
- The insulation layer;  $\lambda = 0.04$  W/m K.
- The concrete structure;  $\lambda = 1.4$  W/m K.
- The right-hand side surface interfaces the environment.

The boundary conditions for the CFD model in Fig. 6 are as follows:

- Fixed temperature of the reactor vessel wall (red surface at the left) for different axial levels ( $T_{vw} = 400, 500, 600,$  and  $700$  °C). This is intended to represent the different levels of the heat source inside the vessel.
- The heat sink is the environment outside of the concrete structure (black surface at the right). As a first approximation, the following data are taken for the heat transfer with the ambient, outside of the concrete structure:  $T_a = 50$  °C and  $\alpha = 6$  W/m<sup>2</sup> K, where  $\alpha$  is the heat transfer coefficient. For later calculations, the heat sinks will include the water cooling system.
- The other outer surfaces, except the interface with the environment (black surface on the right side in the picture), are defined as “symmetric,” i.e., adiabatic.

Calculations were made first without taking into account the oil cooling system in order to see if one could reach, with the only heat removal to the environment, required temperature level in the concrete domain.

**2.4 Analytical Solution for Verification.** The current CFD model without local heat sinks (the cooling systems) is convenient for verification by comparison to an analytical solution. This

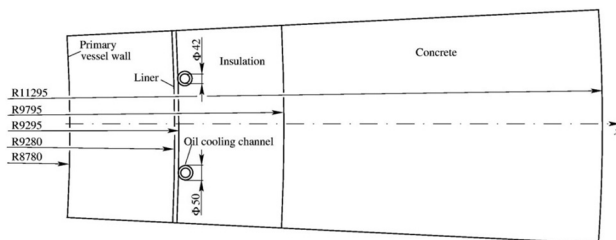


**Fig. 5 Drawing of an elementary cell of the reactor pit model**

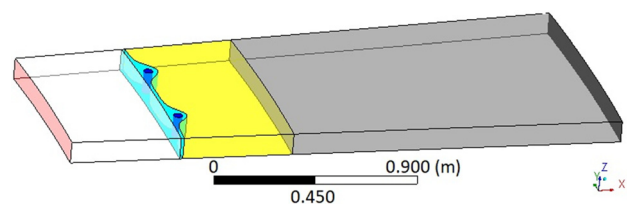


**Fig. 6 The CFD model of an elementary cell of the reactor pit model**

requires one-dimensional model of the heat transfer by radiation in the gap and by heat conduction in the solids. The heat path is from the hot reactor vessel wall toward the outer concrete surface facing the environment. The heat flow due to radiation in the gap between a hot surface (index 1) and a cold surface (index 2) can be written as<sup>3</sup>

$$\dot{Q} = \frac{\sigma(T_1^4 - T_2^4)}{\frac{1 - \varepsilon_1}{A_1 \varepsilon_1} + \frac{1}{A_1 F_{12}} + \frac{1 - \varepsilon_2}{A_2 \varepsilon_2}} \quad (1)$$

Hereby,  $T$  is the (absolute) temperature, and  $\sigma = 5.67 \times 10^{-8} \text{ W/m}^2 \text{ K}^4$  is the Stefan-Boltzmann constant. Assuming emissivity of stainless steel for both surfaces  $\varepsilon_1 = \varepsilon_2 = 0.4$  that is a typical value for stainless steel and full visibility ( $F_{12} = 1$ ) and for  $A_1 \approx A_2 = A$ , the temperature of the cold surface yields

$$T_2 = \left( T_1^4 - \frac{\dot{Q}}{A\sigma} \left( 2 \frac{1 - \varepsilon}{\varepsilon} + 1 \right) \right)^{\frac{1}{4}} \quad (2)$$

Heat conduction through a cylindrical solid wall in direction of the radius  $r$  can be written as

$$\dot{Q} = -\lambda A(r) \frac{dT}{dr} \quad (3)$$

Hereby,  $\lambda$  is the thermal conductivity of the solid, and  $A(r) = 2\pi rh$  the cylindrical surface at the radius  $r$  and for a segment of the height  $h$ . The integration between the radii  $r_1$  and  $r_2$  with the corresponding temperatures  $T_1$  and  $T_2$  yields the temperature at the outer radius

$$T_2 = T_1 - \frac{\dot{Q}}{\lambda} \frac{\ln\left(\frac{r_2}{r_1}\right)}{2\pi h} \quad (4)$$

**2.5 Heat Transfer Assessment Without the Cooling System.** For this computation, the oil cooling channels in the liner in Fig. 6 are not taken into account. The liner is considered to be flat (equal thickness) and without pipes. The temperature along the heat path in the center of the domains is shown in Fig. 7. In Fig. 7(a), the constant-temperature boundary condition is applied at the primary vessel wall ( $T_{vw} = 400, 500, 600$ , and  $700^\circ\text{C}$ , red surface in Fig. 6). In the nearly vacuum domain of the gap, the heat transfer takes place by means of radiation, and the temperature is almost identical to the boundary condition. The temperature of the metal liner is also very close to the temperature of the vessel (since the cooling system is not modeled in this case). As expected, the main temperature drop takes place in the insulation layer. However, the temperature in the concrete is mostly above the required limit of  $70^\circ\text{C}$  as shown in Fig. 7(b). Furthermore, the CFD results are compared with the analytical solutions of Eqs. (2) and (4). The maximum deviation of the temperature is less than  $5^\circ\text{C}$ .

**2.6 Heat Transfer Assessment With the Cooling System.** For this computation, a constant average temperature  $T_{cc}$  at the oil cooling channel walls (see Fig. 5) is set as an additional boundary condition. The aim is to understand the interaction between the reactor vessel wall temperature, the oil cooling system temperature, and the maximum concrete temperature. The final goal is to estimate the power removed by the oil cooling system.

Parametric calculations of the power removed by the oil cooling system for various vessel and oil temperatures were evaluated (see Fig. 8). In the following, an average oil temperature of about

$200^\circ\text{C}$  is proposed as working hypothesis for the reactor operation, in order to be sure to be far below the upper operating range of the Therminol oil ( $315^\circ\text{C}$ ). Additionally, Fig. 9 shows the temperature field for the computed elementary cell. The hot reactor vessel with the constant temperature of the vessel wall equal to  $T_{vw} = 700^\circ\text{C}$  is on the left-hand side. The temperature of the oil cooling channel walls is set to  $T_{cc} = 200^\circ\text{C}$ . Most of the heat transfer takes place between the vessel wall and the cooling channel. Even at the highest considered wall temperature, the maximum concrete temperature is still slightly below  $70^\circ\text{C}$  (concrete integrity criteria).

According to an oil average temperature of approximately  $200^\circ\text{C}$ , the power removed by radiation from the reactor vessel at nominal conditions (see Fig. 8, for  $T_{vw} = 400^\circ\text{C}$ ) is about  $3000 \text{ W/m}^2$ . The surface of the reactor vessel, radiating toward the oil cooling system, is about  $1050 \text{ m}^2$ . Therefore, at nominal operation (cf. scenario 1, Sec. 2.2), approximately 3 MW will be removed.

For scenario 2 (cf. Sec. 2.2) in the exceptional situation of successive losses of DHRS, the reactor pit cooling system can then remove (the main vessel being at  $650^\circ\text{C}$ ), a power of about 15 MW. This value does not take into account the exchanges by gas convection between vessel and liner and could be also increased by special surface treatment of the liner to increase its emissivity coefficient. To be noticed that the value of 15 MW corresponds to the DH power level after about three days.

For scenario 3, we assume now that the oil cooling system is out of operation, but DHRS-1 and DHRS-2 are able to guarantee that the primary sodium is at about  $200^\circ\text{C}$ , so the liner temperature will also be at  $\sim 200^\circ\text{C}$ . Now, for scenario 2, we also assumed that the average oil temperature is at  $\sim 200^\circ\text{C}$ , and found that the liner temperature is approximately in the range  $200\text{--}400^\circ\text{C}$ , see Fig. 9, with no degradation of the concrete pit (temperature below the  $70^\circ\text{C}$  threshold). Therefore, the conducted preliminary analysis based on the use of the oil cooling system alone is potentially applicable to all three scenarios.

In conclusion, two active (forced-convection) cooling systems are proposed: an oil cooling system close to the metallic liner and a water cooling system in the reactor pit concrete structure. The main goals of the cooling systems are to keep the reactor vessel at acceptable temperature level and to maintain the concrete temperature below  $70^\circ\text{C}$  in the three scenarios of operation envisaged (normal operation, DH removal without and with primary sodium leak).

The first calculations showed that if the oil cooling system is designed to keep the liner temperature at about  $200^\circ\text{C}$ , then this system alone can fulfill both goals. At the same time, the water cooling system alone should be able to maintain the concrete temperature below  $70^\circ\text{C}$  in the three scenarios, even if the oil system is lost.

The proposed reactor pit design has several advantages: elimination of the safety vessel, better efficiency of the DH removal by the reactor pit cooling systems, and safer configuration in case of accidental or mitigation situations. Finally, the new reactor pit systems are easier to survey, to inspect, and to repair. However, the general pit architecture proposed remains to be validated, in terms of feasibility, by the manufacturer, and in terms of final acceptance by safety authorities.

### 3 New Decay Heat Removal Systems

The prolonged loss of the DHRS of a sodium fast reactor would have uncontrollable consequences. The creep of the vessel, then its rupture, would lead to core meltdown in a situation where the geometry of the main structures needed for limiting the radiological consequences of the accident, e.g., core catcher, would be degraded. This situation is therefore one of the situations to be practically eliminated. To demonstrate the practical elimination, it is necessary to demonstrate that the probability of a loss of the DHRS is very low with a high confidence level. To arrive to this

<sup>3</sup>Here, the gas convection is not considered. The temperature of the vessel wall is considered to be constant over the height. The intention is to keep this model simple.

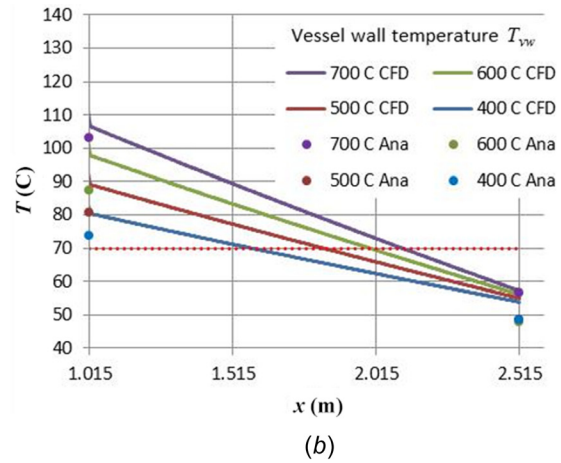
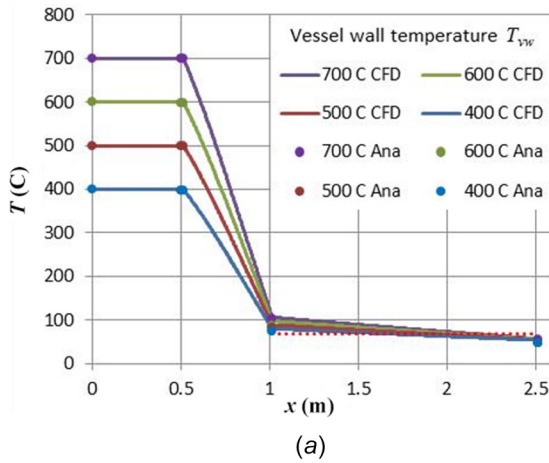


**Fig. 7** The temperature along the heat path (in  $x$  direction); computation (CFD) and analytical solution (Ana); (a) the whole length and (b) the concrete domain. The dotted line denotes the temperature limit of 70 °C.

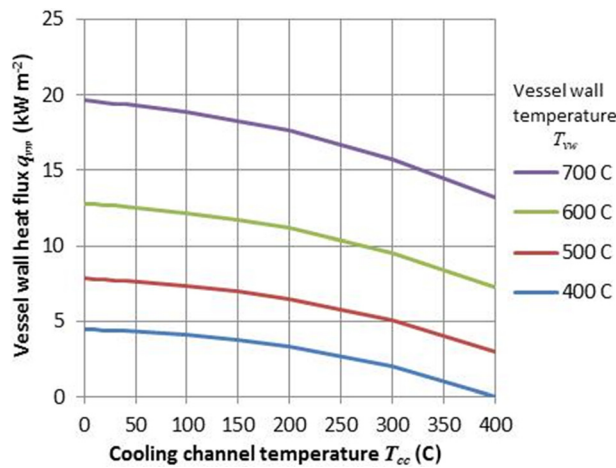


**Fig. 8** Power removed by the oil cooling system at different temperatures of the reactor vessel and the oil cooling channel wall

demonstration, it is generally recognized that the system must have two strong lines of defense and a medium line of defense that are independent. Each line of defense must be able to perform the decay heat removal (DHR) function on its own. This means in a simplified way that it must be able to evacuate about 1% of the nominal thermal power of the reactor, which corresponds to the value of the residual power a few hours after reactor shutdown. The medium line of defense may have a weaker capacity, but must also be able to ensure the DHR function alone some time later after the reactor shutdown when the other DHR systems may

reasonably be postulated to be failed. Finally, these systems have also to be easy to survey, to inspect, and to repair.

The DHR function is provided by three independent systems called DHRS-1, DHRS-2, and DHRS-3, already presented in Ref. [2]. This paper presents precalculations of these three systems to demonstrate their ability to form two strong lines of defense (DHRS-1 and DHRS-2) and a medium line of defense (DHRS-3). Considerations are also given on redundancy and simplicity of plant operation. The proposed set of DHRS allows having a good confidence in the possibility of the global system to meet the new criteria of safety of the Generation-IV reactors. However, it does not constitute a complete safety demonstration, as conducted for a safety authority on a project under construction.

**3.1 DHRS-1.** DHRS-1 consists of six innovative circuits, one per IHX, extracting hot secondary sodium from the IHX, cooling it in an external sodium/air heat exchanger, and returning it to the inlet of the IHX. This system, installed outside of the primary vessel, has many advantages and is designed to extract alone 100% of the DH in a completely passive way.

DHRS-1 draws secondary hot sodium (550 °C during normal operation, with higher temperatures acceptable in accident condition) from the IHX hot plenum at the outlet of the tubular zone (see Fig. 10). This sodium circulates to a sodium/air heat exchanger of DHRS-1 and then back down to the IHX where it is reinjected into the central pipe of the IHX. The maximum height between the hot plenum connection and the highest point of the DHRS-1 loop is design to be 12 m to avoid unacceptable pressure reduction resulting in sodium boiling. A sodium circulation is established in nominal operation in opposite direction because of the loss of charge in the IHX, around 0.2 MPa (200 mbar). When secondary pumps are stopped or work at low rotational speed, the sodium circulation is ensured by the natural convection and the thermal pump installed on the hot leg.

It is necessary to be able to extract 1% of the nominal power, i.e., 36 MW with only five systems (to take in account the rule that one of the system can be out of order), so that the DHRS-1 can be classified as a strong line of defense. That means that each system should be able to extract 7.2 MW. But calculations are provided only for an extraction of 6 MW with sodium at 550 °C, because, in this case, the value of 7.2 MW would be easily reached with a higher temperature of about 580 °C that is admissible. To extract 6 MW with a temperature difference of 400 °C (550 °C/150 °C), a sodium flow of about 15 kg/s is necessary. With the exact physical properties (in particular, the variation of liquid sodium specific heat between 150 °C and 550 °C), we obtain that the flow necessary to evacuate 6 MW between 150 °C and 550 °C is 11.5 kg/s, that means a velocity of 0.4 m/s in the cold leg and

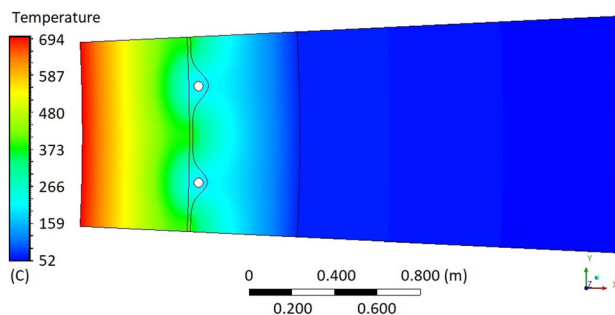


**Fig. 9** Temperature field,  $T_{vw} = 700$  °C, and  $T_{cc} = 200$  °C



0.45 m/s on the hot leg using a pipe of 200-mm diameter. It should be noted that the sodium/air heat exchanger used at the Superphénix SFR had a similar design and was able to extract about 6.4 MW in natural convection [4]. Therefore, the dimensions of the DHRS-1 heat exchanger were proposed to be similar in the ESFR-SMART design. With these dimensions, the pressure loss measured at Superphénix was 0.03 MPa (0.3 bar) for a flowrate of 12.4 kg/s, so about 0.025 MPa (0.25 bar) is expected for the flowrate of 11.5 kg/s selected for the DHRS-1 design. Therefore, a pressure head of about 0.025 MPa (0.25 bar) has to be ensured both by the natural convection and by the thermal pump to guarantee the adequate flowrate using the Superphénix-like heat exchanger.

Concerning the DHRS-1 operation under nominal conditions, the window in the box of the sodium/air heat exchanger is closed, and the sodium remains cold in all the circuit. This cold sodium is reinjected into the IHX hot plenum. A mixing grid will therefore be necessary to avoid mechanical stress due to thermal striping (i.e., fluctuation of the coolant temperature on the wall). This mixing should be easy because the reinjected flowrate is less than 0.5% of the secondary flow. If we want to use the DHRS-1 systems, we need to stop or to operate at low speed the secondary pumps, before we can open the hatches (the blue window in the lower part of the orange chimney in Fig. 11) allowing the air flow enter in the sodium/air heat exchangers casing. Natural convection in DHRS-1, about 0.001 MPa (10 mbar), and thermal pump, about 0.0015 MPa (15 mbar), allow a good sodium circulation with a cold column in the IHX and in a very passive way. The opening of the hatches is regulated by the measurement of sodium temperature leaving the sodium/air heat exchangers that should remain above 150 °C to avoid freezing.

This design of DHRS-1 has several advantages compared to the alternative solution where the DHR systems are located in the primary pool as in Superphénix [4] or in the Collaborative Project (CP) ESFR project [3]:

- No additional penetrations in the reactor roof are required. It is beneficial for reducing the reactor vessel diameter, even though the IHX diameter should be slightly increased to include the 0.2 m diameter pipe of the DHRS-1.
- A column of the cold primary sodium is maintained in the IHX, which is the guarantee of a good natural convection in the primary circuit and in the core (as verified by the

SuperPhénix [4] and Phénix [8] operation experience feedback), which was not the case with systems implemented in the primary pool in some transient situations [4].

- The DHRS-1 circuit uses secondary sodium and therefore already existing sodium purification system of the corresponding secondary loop. This minimizes the number of sodium circuits to be managed by the operator. Indeed, each dedicated system implemented in the primary pool would require a sodium circuit to manage with its own sodium purification system and its own sodium draining system.
- The DHRS-1 design reduces the risk of sodium leak out of the primary vessel.
- DHRS-1 is located out of the primary vessel and is more resilient in case of mechanical energy release in case of severe accident.

DHRS-1 is a strong line of defense of the ESFR-SMART DHRS architecture. It is designed to be able alone to assure very passive DHR.

**3.2 DHRS-2.** The ESFR design embeds a sodium pool-type vessel containing the reactor core and six IHXs [2]. Each IHX is connected to six modular steam generators (SGs) which are located in the casings (Fig. 12). So we have six secondary circuits that will be used for DH removal capability. The feed-water is used for heat removal in normal operation and—if available—can be used for the DHR when needed. This DHR path is called DHRS-2. In case of accidents with loss of feed-water supply, it is possible to remove a part of the DH generated in the core via cooling the SG outer shells by natural convection of air in the casings. This operation needs the opening of windows located at the bottom and the top of each casing. Similar procedure was used in the Phénix SFR for the DHR [8].

Calculations were provided using both theoretical calculations and simulations by the CATHARE code to estimate the power evacuated by natural convection of air in these casings around the shells of the modular SG [9]. Calculations were provided in a “Fukushima situation,” it means without water supply in the SG and without electricity supply for the pumps. Therefore, we use only natural convection of air and sodium. The first calculations made without chimneys above the casings show that with the DHRS-2 alone the temperature reached by the primary sodium is too high in regard of the criterion of a maximum transient

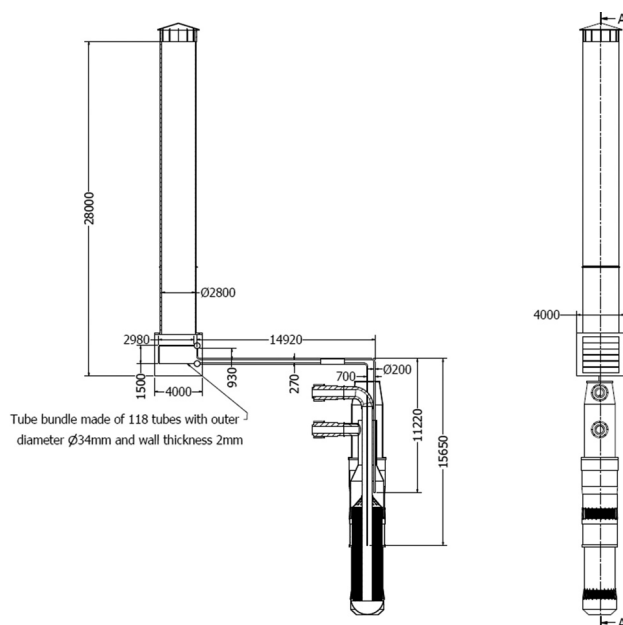


Fig. 10 Drawings of DHRS-1

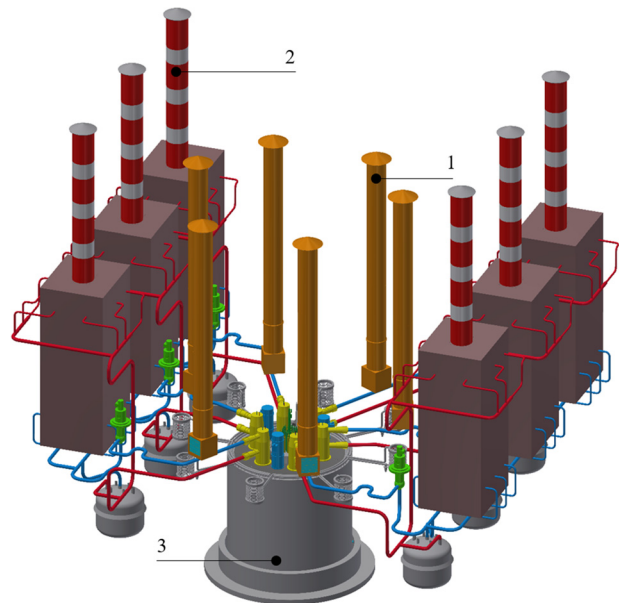


Fig. 11 ESFR-SMART main view of the reactor with the three DHR systems: 1—DHRS-1, 2—DHRS-2, and 3—DHRS-3

temperature of 650 °C. Calculations provided with chimneys above the casings show a clear improvement in air heat removal capabilities. This design is retained for the final design of the reactor (Fig. 11). However, the maximal transient temperature remains too high (about 700 °C) with the DHRS-2 alone. To reach maximal transient temperatures below 650 °C, the operation of DHRS-3 should be taken into account. On the other hand, if the pumps can ensure secondary sodium circulation, DHRS-2 alone can guarantee the DH removal, and the maximal sodium temperature at the core outlet will remain under 650 °C.

In conclusion, if the sodium flow is maintained in the secondary loops, DHRS-2 is designed to be able to ensure alone the DHR function. In case of Fukushima situation (i.e., without feed-water and without electricity supply), the natural convection of secondary sodium is however not sufficient to ensure alone the DHR function. It is necessary to take in account the DHRS-3 contribution to safely ensure the DHR.

Finally, emergency diesel generators allow DHRS-2 to cope with the loss of external electrical supply and to be considered as a strong line of defense of the ESFR-SMART DHRS architecture. The six circuits assure redundancy possibilities.

**3.3 DHRS-3.** One of the options analyzed in the ESFR-SMART project is the elimination of the second (safety) vessel and to use the reactor pit for withstanding sodium leakage from the primary vessel. In the reactor pit, an oil cooling system is installed between the primary vessel and the liner. The system is used for cooling the reactor pit in normal operation and can be used for DHR when needed. This heat removal path is called the DHRS-3 [10]. The elimination of the safety vessel that shields the heat removal substantially increases the DHR capabilities of the DHRS-3. The calculations made show that with a sodium temperature of 650 °C the oil circuit can extract about 15 MW [11] (see Fig. 8 and Secs. 2.1–2.6).

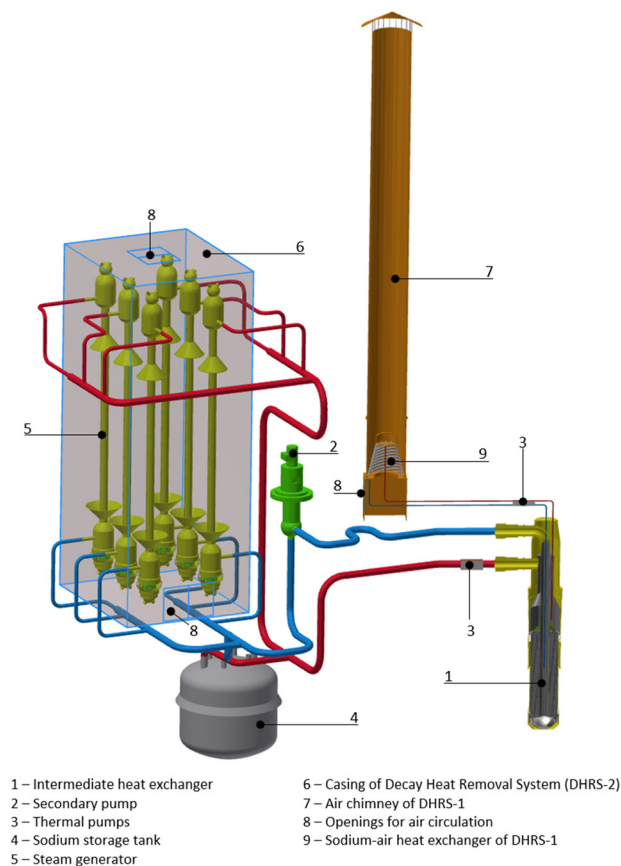


Fig. 12 Secondary sodium loop with DHRS-1 and DHRS-2

The DHRS-3 consists of several independent oil systems to ensure redundancy. Approximately three days after the reactor shutdown, the DHRS-3 is capable alone to ensure the DH removal. After this time, DHRS-3 can be considered as a strong line of defense.

Indeed, if DHRS-3 is redundant, it can be defined as a strong line of defense. But, the efficiency of DHRS-3 is sufficient when the decay heat is sufficiently low (about three days). Therefore, it will be necessary to justify that the early failure of both DHRS-1 and DHRS-2 is not credible. This is judged possible taking into account the high level of redundancy of DHRS-1 and DHRS-2 combined with their capability to operate in natural convection.

**3.4 General Operation of the Reactor.** The ESFR with the three DHR systems is shown in Fig. 11. It should be noted that the operation of the DHR systems is expected to be simple for the operator. After the reactor shutdown, the secondary loops very easily ensure the DH removal. In the event of loss of the water supply, the operator of the control system of DHRS-2 opens the windows of the steam generator casings, ensuring the secondary sodium cooling thanks to the natural convection of the air around these steam generators. During this time, the oil heat removal system in front of the reactor vessel ensures a non-negligible complement and is designed to be able after about three days to ensure this function alone. If these circuits become unavailable, the operator of the control system of DHRS-1 opens the windows of sodium/air heat exchangers of the DHRS-1. The natural convection of secondary sodium in this loop then allows the DHR in a completely passive way by maintaining a column of the cold primary sodium in the IHX and thus a good natural convection of primary sodium through the core.

The three systems are redundant and diversified: six loops for the DHRS-1, six secondary loops for the DHRS-2, and several independent oil circuits for the DHRS-3. At least two of them systems have a lot of passivity (DHRS-1 and DHRS-2) and are easy to operate. They are robust, resilient, and admitting significant grace periods due to the high thermal inertia of the primary pool circuit.

In conclusion, the analyses and preliminary calculations carried out on the three DHR systems of the European Sodium Fast Reactor seem to give a good confidence on the heat removal safety function according to the safety rules for the Generation-IV reactors. It should also be noted that the ESFR-SMART project aims at simplifying the reactor operation for the operator with the use of simple, passive, redundant, and forgiving systems.

## 4 Core Catcher System

The use of a core catcher able to retain the corium of a melted SFR core is required by safety authorities. The first SFR built, as, for example, Phénix, did not have core catcher. One of the first SFR to have this type of mitigation device was Superphénix (Fig. 13).

The last SFR built and operated is the BN-800 reactor in Russia (in operation since 2017) features a core catcher installed in the reactor under the diagrid. In this core catcher, the upper part is covered with molybdenum, a sodium-compatible material with a very high melting point (2623 °C) and excellent thermal conductivity. After assembly, chimneys also protected by molybdenum are installed to allow a good circulation in natural convection of sodium cooling the lower part of the device, to extract the downward thermal flux.

In the previous CP-ESFR project, the analyses showed, under conservative assumptions regarding heat transfer, that cooling could be ensured for ~10% of the total corium mass. Therefore, to improve the internal core catcher mass retention and heat dissipation capacity, several studies have been conducted in the frame of the ESFR-SMART project. These studies are shown in this paper with a new design proposition.



**4.1 Severe Accident Conditions.** The ESFR-SMART core concept with lower void effect features a better behavior in case of severe accident scenarios than the previous cores (e.g., the core designed in the frame of the CP-ESFR project). Moreover, we have in the ESFR-SMART core dedicated tubes for corium discharge that should allow discharging quickly the melted core and should help to prevent criticality. Calculations show that after several seconds, these discharge tubes begin to open, and the corium arrives by this preferential way on the core catcher, quicker, and in limited quantities at the beginning of the accident.

However, things are not trivial, because there could be a strong interactions between liquid corium around 3000 °C and liquid steel around 1500 °C, with sodium. This can even lead to situations where the corium could solidify before reaching the core catcher. R&D is very active in this area, aimed to improve the knowledge of these complex interactions phenomena.

**4.2 Choice of Material for the Core Catcher.** The core catcher must be equipped with a refractory material to which a number of properties are required: Compatibility with sodium (for 60 years), good mechanical resistance during a thermal shock, high melting point, good resistance to erosion under a corium jet, easy to machine or to weld, available, affordable. Reactor experience would be a plus, as well as minimal R&D necessary. The ideal material does not exist, but molybdenum meets a number of these parameters:

- It is totally compatible with sodium (it was used for sodium sample collection in Phénix because it does not pollute sodium).
- With its low coefficient of expansion and high modulus of elasticity, this metal has the best behavior during local thermal shock.
- Its melting and boiling points are extremely high: 2600 °C and more than 4000 °C, respectively, which makes it close to ceramics.
- It has a behavior comparable to ceramics under a jet of molten corium (but worse for a jet of molten metal).
- It is possible to machine or weld it (except some nuances).
- It is available and currently its price is decreasing because of stocks increasingly important (by-product of copper mines), currently its price is around 20 €/kg.
- There is experience of its use in sodium, since it is used for BN-800 and therefore currently in sodium, for example, in Phénix in the sample collection system.

But two negative points should be addressed:

- Molybdenum has been selected for investigation because and despite its high conductivity. This high conductivity is

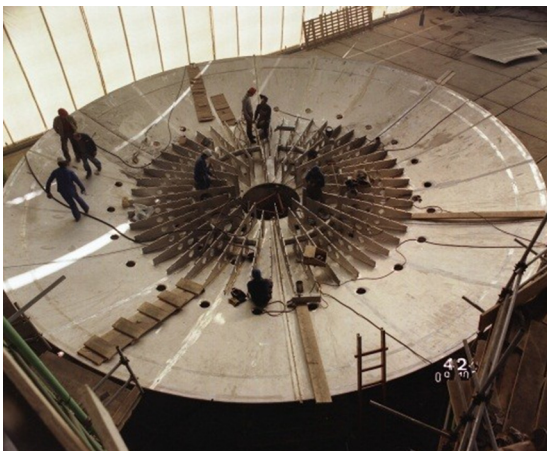


**Fig. 13 View of the Superphénix core catcher under building**

favorable to increase the thermal exchanges. However, this high conductivity with also increase the downward thermal flux toward the sodium below the core catcher. In case of sodium boiling below the core catcher, its coolability could be degraded. Therefore, the design was proposed to improve the natural circulation of sodium below the core catcher.

- The other negative point is the possible creation of a molybdenum-steel eutectic, at high temperature (1450 °C), that could arise when a jet of pure liquid steel impact to core catcher. However, if at the beginning of the core melting sequence, liquid steel may interact with the core catcher, the strong interaction with sodium should lead to steel jet fragmentation and solidification. So that any interaction between a liquid steel jet and the metallic core catcher at high temperature would become very difficult or lasting a very short time.

**4.3 European Sodium Fast Reactor Safety Measures Assessment and Research Tools Core Catcher Concept.** Theoretically, the core catcher could be installed in the primary vessel or directly in the pit. Due to geometrical reasons, in pool-type reactors, sufficient place exists in the primary vessel between the diagrid, the strongback, and the vessel for spreading out the corium and then reducing the risk of criticality and reducing the downward thermal flux. So, this core catcher is installed in this available volume. The option of a core catcher inside the pit itself has not been studied in the ESFR-SMART project.

Figure 14 shows in green the position of the core catcher studied in ESFR-SMART, while Fig. 15 gives an artistic view of the preferential path for the corium (in yellow) moving from the core region to the core catcher (in green), through the discharge tubes (in dark gray).

These corium discharge tubes, coming from the core, emerge above the core catcher to channel the molten corium. Cylinders with conical top endings are installed under these tubes to allow a good dispersion of the corium inside this core catcher (Fig. 15) and to avoid or minimize local ablation, during transitory periods. The volume available in the core catcher allows receiving the whole core fissile inventory. General design of the strongback structures should be designed to allow a good circulation of the sodium above and under the core catcher, to improve cooling by sodium natural convection. The general design allows a good circulation of the sodium under the core catcher, to be able to participate actively to the cooling of the component.

Two options remain open:

- The first calculations with only 25% of molten core show no risk of recriticality of the corium. The disposition of hafnium-type poisons in the lower part of the discharge tubes could be used, if necessary, to increase the margin to criticality.
- We can replace the cylinders by chimneys (Fig. 16) to improve the natural convection of sodium under the core catcher, flowing through the chimneys (as in the BN-800 design).

**4.4 Residual Power of the Melted Core.** One of the key parameters is the power generated by the corium and its decay with time. This power has been calculated with EVOLCODE [12] when considered the CONF2-HET2 core proposed in the CP-ESFR [3] given that at the date of the beginning of this task, the ESFR-SMART core design was not completed. Table 1 presents the power generated by the corium at the given time as well as the power density, obtained as the ratio between the power and the total volume of the corium.

The calculations were performed assuming that corium is at the thermal equilibrium state. The heat transfers before the equilibrium state are not calculated. Two simulations were done

assuming the equilibrium state is achieved 120 s or 1200 s after the beginning of the corium subcriticality.

**4.5 Thermal Calculations.** In order to perform calculations related to the coolability of the core catcher, it has been necessary to develop an algorithm (or code) that solves the heat equation in two dimensions.

A verification of this code with a one-dimensional analysis has been provided with an example of a multilayer core catcher formed by Mo, thoria, and stainless steel as in Ref. [13]. The comparison shows in this case a good agreement.

Calculations have been provided in two cases, with the same hypothesis of a multilayer core catcher as in Ref. [13] and with a core catcher in one molybdenum layer.

Main hypotheses are following:

- diameter of the core catcher equal to 8.7 m;
- corium volume of  $31.4 \text{ m}^3$ ;
- dynamic calculation of the convection coefficients above the corium and below the core catcher according to Ref. [14]; and
- corium considered as a liquid homogeneous mixture of fuel and cladding.

The results are obtained assuming a constant conductivity.

As referred in Ref. [14], the convection coefficients have addressed a 25% uncertainty, so the value employed in the calculation is 0.75 times the calculated convection coefficient. The conductivity of the corium is not that from the fuel, using instead the conductivity reported in Ref. [15] for the corium, whose value is  $7.15 \text{ W/m K}$  considering the uncertainty of the measurement. Additionally, the heat transfer coefficient through the vertical walls is obtained from Ref. [16].

The results show that the total amount of corium mass able to be cooled without sodium boiling by a molybdenum core catcher is reduced with respect to the multilayer core catcher (from 35% in the multilayer core catcher to 25% in the molybdenum core catcher) [17]. However, the limitation to avoid sodium boiling under the core catcher is not useful. A core catcher in one layer is simpler to fabricate and less expensive than a multilayer concept. On the other hand, we avoid all difficulties related to the mechanical behavior of several materials together able to support thermal shocks. The sizing calculations of a component with only one material will be easier. The multilayer design limits the thermal evacuation possibilities without real benefit. Therefore, we propose a core catcher in one layer in molybdenum.

So as any modern SFR projects, the ESFR-SMART project has a core catcher inside the primary vessel, under the diagrid and the strongback. Its function, in case of severe accident with core melting, is to retain the corium and to cool it only with the natural convection of sodium around it. The design of the core catcher takes also advantage of the discharge tubes arriving from the core above this core catcher. Conservatively, we took the option of a core catcher geometrically able to retain the whole melted core. Preliminary thermal calculations were provided with a multilayer and a one-layer concept. The global mechanical behavior of the multilayer concept seems difficult, and there is no clear thermal

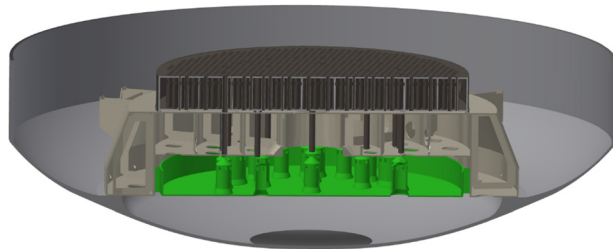


**Fig. 14 View of the core catcher position inside the primary vessel**

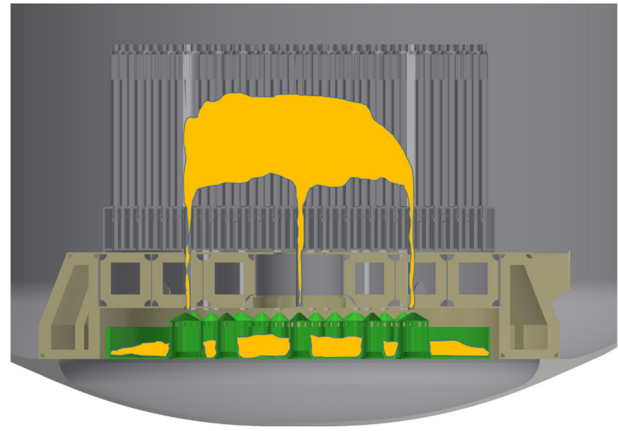


**Fig. 15 “Artistic view” of the preferential ways for the melted core**

advantage. Therefore, we propose a one-layer core catcher in molybdenum, material compatible with sodium and used on the core catcher of the last SFR, started in 2016, BN-800.

With the proposed design, the residual power of the corium can be dissipated by natural convection by sodium circulating around and above the core catcher. Conservative calculations show that even if 25% of whole core is on the core catcher, there is no boiling of sodium under the core catcher. In case of bigger quantities of melted core, boiling of sodium could appear at the lower face of the core catcher. The chimneys (see Fig. 16) will improve the natural circulation of sodium located under the core catcher, but the calculation of this improvement has not yet been made. This residual power will quickly decrease, and sodium natural convection around this core catcher will allow a good general mitigation situation.

## 5 Thermal Pumps

Thermal pumps are passive systems that create motor force in sodium only using temperature difference (described in Refs. [2] and [3]).

The calculations made on the residual power evacuation systems showed that their use on the secondary circuits of the ESFR-SMART project did not provide sufficient gain compared to natural convection. So they were not included in the design of the main secondary circuits.

However, their installation on the DHRS-1 loop would replace an electromagnetic pump and bring passivity to the system (see Fig. 17 showing the principle of the thermal pump operation).

First calculations (Figs. 18 and 19) were conducted with the following parameters:

- pipe diameter 0.2 m
- sodium velocity 0.6 m/s
- temperature difference 300 K (400–700 K)
- chromel/alumel as thermocouples materials

These calculations show the theoretical possibility to reach the pressure head needed to operate passively the DHRS-1 system.

Research and development with test scale 1:1 would be necessary to confirm the operational characteristics of the system.

On the other hand, an electromagnetic pump with an emergency power supply could be used to assure the function if the validation of the thermal pump system is not available.

## 6 Optimization of the Secondary Loops

Finally, the major factor of cost difference between sodium and water reactors is the existence of secondary circuits. A work optimization of the sizes of these circuits is, therefore, necessary not

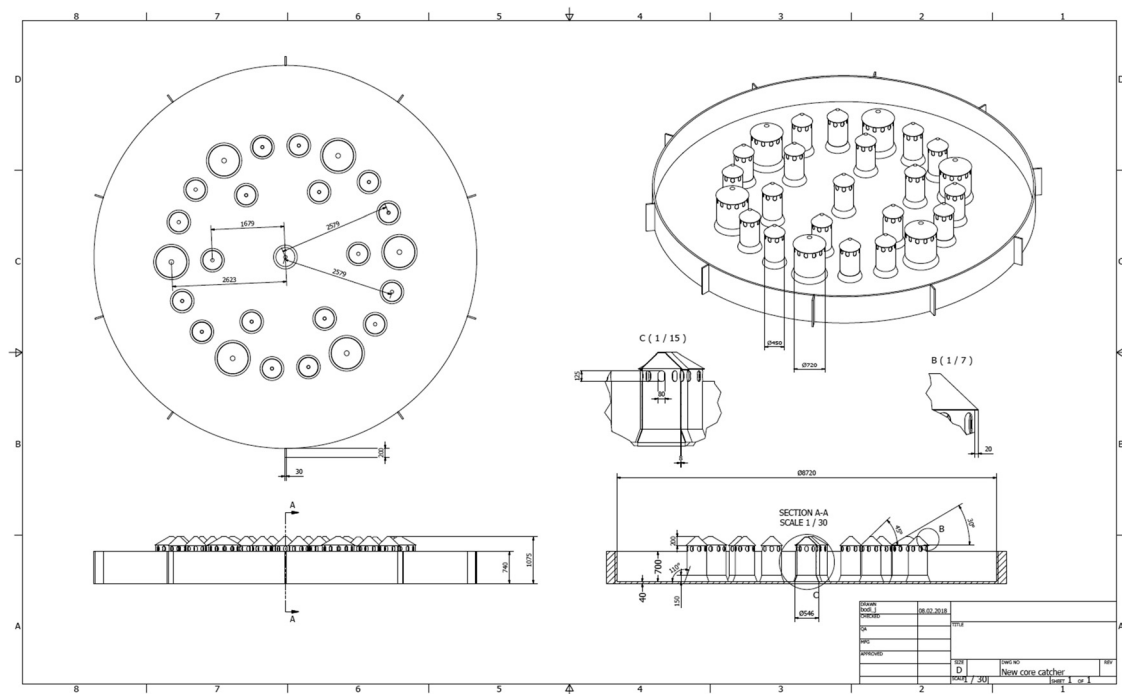


Fig. 16 Drawings of the core catcher with chimneys

only for the circuits but also for the optimization of the secondary building size.

On Superphénix, the sodium pipes were equipped with U-shaped expansion devices to resume the dilations between cold state and operation. However, the heavy weight of these pipes requires supports. It is therefore necessary that the pipes can slide in these supports. However, antiseismic standards require that these pipes be firmly held during earthquakes, leading to the definition of rather complex systems. Finally, after each transient, the pipework was found in unpredicted positions [3]. Another thing that worked poorly was the thermal insulation on these flexible pipes. This led to difficulties in detecting leaks, risks of corrosion by undetected leaks, and numerous false alarms that were very difficult to verify.

Based on this negative feedback in terms of investment (significant extra) and safety (risk of rupture of the piping blocked in their support, and risk of pipes corrosion), the ESFR-SMART project has proposed to define fixed and nonsliding supports, which plays their support role in normal operation and in case of earthquake. Between these fixed points, the pipes are straight. A bellows is installed in the middle of this straight part, which withstands the dilatation effect. A choice of material other than 316L like 9Cr would also significantly reduce this dilatation. It should be noted that the Russian BN-1200 project chose this bellows option.

The benefits are as follows:

- decrease of the costs because decrease of the lengths of pipes, quantities of secondary sodium, volumes of the storage tanks, etc.;
- simpler, cheaper, and more efficient supports, safety gain, simplicity of managing in operation;
- ability to use a removable insulation easy to install on these straight parts and without direct contact (improved detection possibilities, less false alarms, and improved safety);

Table 1 Decay heat generated by the corium several time steps after the reactor shutdown

Time (s)	0.1	1	10	120	600	1200
Power (MW)	427.8	394.9	273.0	176.4	133.8	115.1
Power density (MW/m <sup>3</sup> )	13.62	12.26	8.693	5.617	4.262	3.667

- improvement of the circuit's natural convection with shorter lines; and
- reduction of the distance between fixed points and so of dimensions and cost of secondary building.

In practical terms, on the drawings, we will draw straight pipes to join the fixed points that are the components: exchangers, SG, pumps, DHRS-1, etc. It should be noted that this was already the

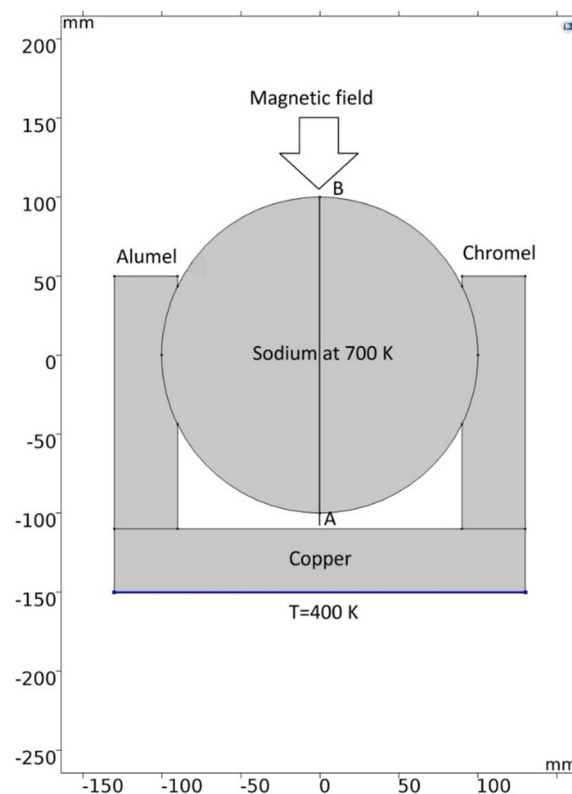


Fig. 17 Principle of thermal pump



case implicit for the exchanger. DHRS-1 connection currently carried out by two straight pipes and without U-shaped thermal expansion devices.

With this option, we manage to reduce the length of the 0.85 m pipes from 220 m to 120 m, and then the volume of sodium inside these pipes decreases from 116 m<sup>3</sup> to 57 m<sup>3</sup>. There is also a big benefit on the final sizing of the secondary building including all pipes and components.

In addition, the mechanical dimensioning of the pipes is simpler because the flexibility option required small thickness of the pipes and numerous welds for the elbows and U-shaped thermal expansion devices. With straight piping, we can minimize the number of welds and take the desired thickness for pipes sizing.

The option of straight lines without elbows allows the use of protection against leakage by a double wall piping (Fig. 20). This installation would be difficult (almost impossible) on large flexible pipes with significant movements. The external wall is internally covered with insulation, and there is a gap between the sodium pipe and this insulation. This external wall can be easily open to allow interventions, for example, in case of alarm.

Classical sodium fire detection is installed on the sodium pipe to detect any leak. These detections are particularly installed around the bellows and in the lower part. Therefore, a sodium leak detection is possible before any chemical interaction of the

sodium with the insulation. Complementary detections can be added between the pipe and the removable insulation, as sodium smoke detection in the partitioned interior zone. This set of provisions allows quick detection and good containment of any sodium leak inside this double wall.

Some R&D is necessary for these bellows of diameter 0.85 m in terms of dilatation capacity and time life. However, the use of bellows in sodium environment is not very new. These bellows existed on many sodium valves especially in Phénix and Superphénix and inside the Phénix heat exchangers. A bellow of large diameter (approximately 0.8 m) was installed in Superphénix (Fig. 21) on the internal part of the hot collector of the intermediate

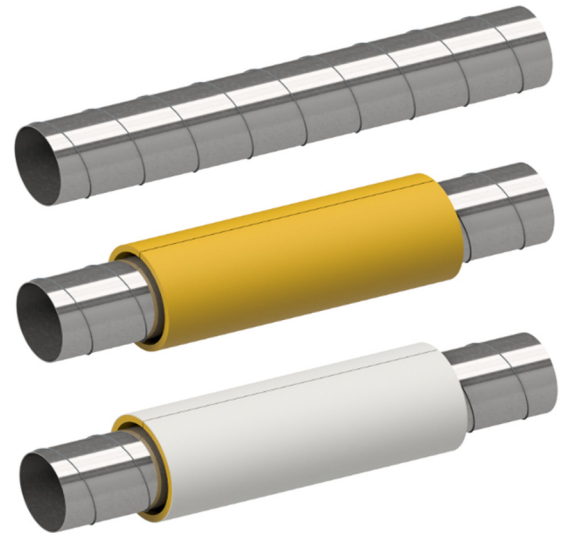


**Fig. 20** View of the straight tube with its external and removable insulation

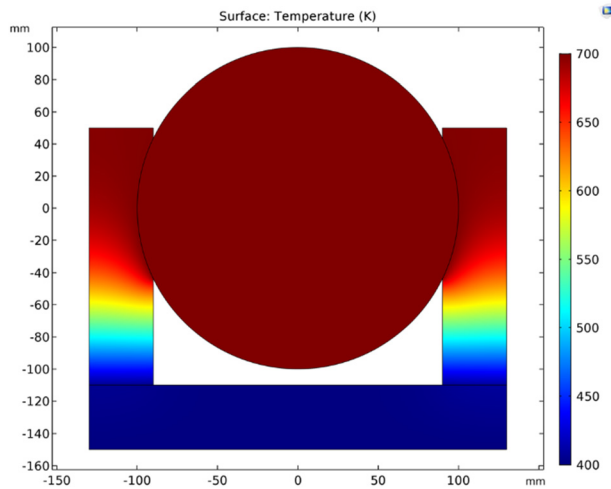


**Fig. 18** Computed temperature in thermal pump—Temperature field (K)

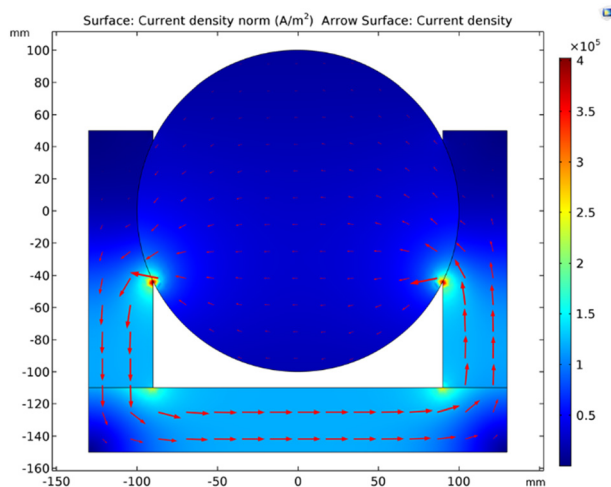


**Fig. 19** Computed current density in thermal pump (A/m<sup>2</sup>)



**Fig. 21** View of the bellow tested on Superphénix heat exchanger

exchangers to take up the differential expansions with the external part. This device had several expansion waves and a thickness of 8 mm. It has undergone a cycling test with a large number of cycles for validation. On the ESFR-SMART steam generator module itself, there is a bellow of large diameter (0.75 m) to allow relative dilatation between the external wall of the SG and its internal bundle.

## 7 Conclusion

This paper provided an overview of the main new safety options for the ESFR-SMART project. A preliminary work was conducted in order to assess the validity of those new safety measures. The main conclusions are:

- For the elimination of the safety vessel, the pit design proposed seems able to withstand a sodium leak of the primary vessel. The thermal calculations show that in all the analyzed cases it seems possible to maintain the primary vessel and the pit concrete under the maximal authorized temperatures.
- For the DHR systems, the calculations show that we have two strong lines of defense able alone to assure 100% of the DHR. One of them, the DHRS-1 is totally passive. These two lines have necessary redundancy. Then, the DHRS-3 is a medium line of defense able after three days to assure alone the DHR. So the criteria necessary to assure the practical elimination of the loss of DHRS lines are fulfilled.
- For the core catcher, first conservative calculations show that it is able to cool at least 25% of the molten core without boiling of sodium under the core catcher. More precise calculations would be necessary to take in account the natural convection of sodium inside the chimneys of the core catcher and to give the quantity of melted core that could be cooled by natural convection of sodium.
- For the thermal pumps, first calculations show the theoretical possibility to reach the wanted characteristics.
- In addition, for the secondary loops, the advantages of bellows in final design have been explained and quantified.

In conclusion, this work did not show impossibilities or big uncertainties, which may question the options proposed. However, the final validation in an industrial project of all these options would need further R&D work, including:

- industrial validation of the pit design construction;
- final design of oil system in front of the main vessel;
- calculation of the core catcher thermal hydraulic behavior with chimneys;
- test of the DHRS-1 thermal pump to validate its characteristics; and
- R&D on bellows behavior for secondary loops optimization.

## Acknowledgment

The work has been prepared within EU Project ESFR-SMART.

## Funding Data

- EURATOM Research and Training Programme 2014–2018 (Grant Agreement No. 754501).

## Nomenclature

Ana = analytical solution  
 ansys cfx = finite elements CFD software tool  
 BN-1200 = Russian design of sodium-cooled fast breeder reactor  
 BN-800 = Russian sodium-cooled fast breeder reactor, built at the Beloyarsk Nuclear Power Station  
 CFD = computational fluid dynamics

CONF2-HET = core design from CP-ESFR project

CP = Collaborative Project

DH = decay heat

DHR = decay heat removal

DHRS-1 = passive decay heat removal system connected to IHX

DHRS-2 = passive decay heat removal system connected to secondary loop

DHRS-3 = active decay heat removal system located in the reactor pit

ESFR = European Sodium Fast Reactor

IHX = intermediate heat exchanger

R&D = research and development

SFR = sodium fast reactor

SG = steam generator

SMART = Safety Measures Assessment and Research Tools

## Symbols

$A$  = reactor vessel cylindrical wall surface,  $m^2$   
 $h$  = reactor vessel cylindrical height, m  
 $q$  = average reactor vessel wall heat flux,  $W/m^2$   
 $Q$  = total reactor vessel wall heat transfer rate, W  
 $r$  = radial coordinate in the reactor pit, m  
 $T$  = absolute temperature, K  
 $T_a$  = ambient temperature,  $^{\circ}C$

## Greek Symbols

$\alpha$  = heat transfer coefficient,  $W/m^2 K$   
 $\varepsilon$  = emissivity  
 $\lambda$  = thermal conductivity,  $W/m K$   
 $\sigma$  = Stefan–Boltzmann constant,  $W/m^2 K^4$

## Subscripts

cc = cooling channel  
 el = electric  
 vw = reactor vessel wall

## References

- [1] Mikityuk, K., Girardi, E., Krepel, J., Bubelis, E., Fridman, E., Rineiski, A., Girault, N., Payot, F., Buligins, L., Gerbeth, G., Chauvin, N., Latge, C., and Garnier, J. C., 2017, “ESFR-SMART: New Horizon-2020 Project on SFR Safety,” Proceedings of the International Conference on Fast Reactors and Related Fuel Cycles: Next Generation Nuclear Systems for Sustainable Development (FR17), Yekaterinburg, Russia, June 26–29, Paper No. *IAEA-CN245-450*.
- [2] Guidez, J., Bodi, J., Mikityuk, K., Girardi, E., and Carlucci, B., 2021, “New Reactor Safety Measures for the European Sodium Fast Reactor—Part I: Conceptual Design,” *ASME Paper No. NERS-20-1059*.
- [3] Fiorini, G. L., and Vasile, A., 2011, “European Commission—7th Framework Programme. The Collaborative Project on European Sodium Fast Reactor (CP ESFR),” *Nucl. Eng. Des.*, **241**(9), pp. 3461–3469.
- [4] Guidez, J., and Prêre, G., 2017, *Superphénix. Technical and Scientific Achievements*, Atlantis Press, Paris, France.
- [5] Therminol, “Therminol® SP Heat Transfer,” accessed July 23, 2021, <https://www.therminol.com/products/Therminol-SP>
- [6] Therminol, “Therminol® Selection Guide,” accessed July 23, 2021, <https://www.therminol.com/sites/therminol/files/documents/TF8691.pdf>
- [7] ANSYS, “ANSYS CFX,” accessed July 23, 2021, <https://www.ansys.com/products/fluids/ansys-cfx>
- [8] Guidez, J., 2014, *Phénix Experience Feedback*, EDP Sciences, Les Ulis, France.
- [9] Bittan, J., Boré, C., and Guidez, J., 2020, “Preliminary Assessment of Decay Heat Removal Systems in the ESFR-SMART Design: The Role of Natural Air Convection Around Steam Generator Outer Shells in Accidental Conditions,” *ASME Paper No. NERS-20-1079*.
- [10] Guidez, J., Bodi, J., Mikityuk, K., Rineiski, A., and Girardi, E., 2018, “New Safety Measures Proposed for European Sodium Fast Reactor in Horizon-2020 ESFR-SMART Project,” GIF Symposium, Paris, France, Oct. 16–17, pp. 1–14.
- [11] Guidez, J., Gerschenfeld, A., Girardi, E., Mikityuk, K., Bodi, J., and Grah, A., 2019, “European Sodium Fast Reactor: Innovative Design of Reactor Pit Aiming at Suppression of Safety Vessel,” Proceedings of the International Congress on Advances in Nuclear Power Plants (ICAPP 19), Juan-les-Pins, France, May 12–15, Paper No. 280.
- [12] Álvarez-Velarde, F., González-Romero, E. M., and Rodríguez, I. M., 2014, “Validation of the Burn-Up Code EVOLCODE 2.0 With PWR Experimental Data and With a Sensitivity/Uncertainty Analysis,” *Ann. Nucl. Energy*, **73**, pp. 175–188.

- [13] Sudha, A. J., Velusamy, K., and Chellapandi, P., 2014, "A Multi Layer Core Catcher Concept for Future Sodium Cooled Fast Reactors," [Ann. Nucl. Energy](#), **65**, pp. 253–261.
- [14] Le Rigoleur, C., and Tenchine, D., 1982, "Sodium Natural Convection Heat Transfers Around the Internal Core Catcher in Super Phenix 1. Experimental Results and Evaluation for Reactor Conditions," International Topical Meeting on Liquid Metal Fast Breeder Reactor Safety and Related Design and Operational Aspects, Lyon, France, July 19–23, pp. 1–14.
- [15] Sparrow, E. M., and Gregg, J. L., 1959, "Details of Exact Low Prandtl Number Boundary-Layer Solutions for Forced and for Free Convection," NASA, Washington, DC, NASA Memo 2-27-59E.
- [16] Mukhamedov, N., Skakov, M., Deryavko, I., and Kukushkin, I., 2017, "Thermal Properties of Prototype Corium of Fast Reactor," [Nucl. Eng. Des.](#), **322**, pp. 27–31.
- [17] Díaz-Chirón, U., Romojaro, P., and Álvarez-Velarde, F., 2019, "Preliminary Calculations of the ESFR Core Catcher," CIEMAT, Madrid, Spain, Internal Report No. DFN/IN-01/II-18.